J. Electroanal. Chem., 283 (1990) 319–336
Elsevier Sequoia S.A., Lausanne – Printed in The Netherlands

Modulated reflectance spectroscopy and voltammetry of the sulphide/gold system

R.O. Lezna, N.R. de Tacconi and A.J. Arvia

Instituto de Investigaciones Fisicoquímicas Teóricas y Aplicadas (INIFTA), Facultad de Ciencias Exactas, Universidad Nacional de La Plata, Sucursal 4, Casilla de Correo 16, 1900 La Plata (Argentina)

(Received 10 January 1989; in revised form 27 October 1989)

ABSTRACT

The electroadsorption of sulphide species on gold and the growth of sulphur multilayers have been investigated by optical and electrochemical techniques in sodium tetraborate buffer as the supporting electrolyte (pH 7.0 and 9.2) at 25°C. Differential reflectance spectra indicate that the adsorption of sulphide begins inside the hydrogen evolution reaction (HER) region. The HER is catalysed by the presence of sulphide species on the electrode. During the growth of sulphur multilayers, soluble polysulphide species can be optically detected either as intermediates under diffusion-controlled kinetics or as products of a chemical reaction between sulphide ions and the deposited sulphur layer. The steep fall in the integral reflectance at 0.4 V (vs. SHE) is interpreted through the incorporation of light-absorbing polysulphides into the structure of the deposited sulphur layer.

(I) INTRODUCTION

The interactions of sulphide-containing species with different electrode materials have been the subject of many investigations [1–15] covering the range from general basic aspects of electrochemistry to practical problems. The importance of sulphur-containing layers is relevant to different electrochemical systems. Thus, the sulphur-containing layers which can be formed on different metal surfaces usually change considerably the energetics of the reactions taking place on those surfaces. An example of this behaviour is found in the electrochemical formation of a methylene blue monolayer on a sulphur-modified gold electrode [16]. In this case, the sulphur layer increases the reversibility of the electron transfer taking place at the first monolayer of methylene blue. On the other hand, sulphur layers can alter drastically the stability of a metal in contact with a sulphide-containing environment, by changing the resistivity at the metal/solution interphase, by modifying the electrode surface wetting properties, or by creating conditions for localized corrosion [17]. Furthermore, in photoelectrochemical cells, sulphide ions in solution can

0022-0728/90/$03.50

interact strongly with cadmium chalcogenides, improving the behaviour of photoelectrodes [9].

The present work is devoted to investigating the electrosorption of sulphide species on gold and the growing conditions for sulphur-containing multilayers, by combining in-situ visible reflectance spectroscopy and electrochemical measurements.

(II) EXPERIMENTAL

Optical measurements were made with a specially designed visible reflectance spectrometer assembled in our laboratory for in-situ studies of electrochemical systems. The details of this set-up as well as those of the electrochemical cells have been described elsewhere [18].

The working electrode was a gold disc (Specpure, Johnson Matthey, 7 mm diameter) encased in Kel-F, polished to a mirror finish with alumina of different grain sizes and cleaned of remaining particles in an ultrasonic bath before being placed into the cell. The working electrode was potential-cycled in the supporting electrolyte between about -0.7 V (vs. SHE) and 0.5 V, at 0.02 V/s before adding sulphide to the electrochemical cell. The potential of the working electrode was measured against a saturated calomel electrode, but in the text all potentials are referred to a standard hydrogen electrode (SHE). Electrochemical experiments were carried out in a conventional way. All experiments were performed under nitrogen at 25 °C, using sodium tetraborate buffer solutions as the supporting electrolyte. In order to analyse the influence of pH on the mechanism of multilayer formation, buffers of pH 7 and pH 9.2 were selected. Solutions of pH 7 were prepared from 0.195 M $Na_2B_4O_7$ + 0.097 M H_2SO_4, and 0.050 M $Na_2B_4O_7$ was used for pH 9.2. The sulphide solutions were prepared just before running each experiment by dissolving $Na_2S \cdot 9\ H_2O$ (Merck p.a.) in the deoxygenated buffer solution.

(III) RESULTS

(III.1) Voltammetric data

Voltammograms run at 0.02 V/s for a gold electrode in solutions containing different concentrations of sodium sulphide at pH 7 and 9.2 are shown in Figs. 1a and 1b. Blank voltammograms are also included for comparison. The potential was scanned from -0.68 V (at 7 pH) and -0.74 V (at pH 9.2) covering different potential amplitudes. For pH 7, and at low positive potential limits, the positive-going potential scan shows only a single current peak (A_1) followed by a shoulder (A^*) at ca. -0.35 V. The reverse scan displays the complementary cathodic peak (C_1), and subsequently, the onset of the HER shifted to more positive potentials with respect to that of the blank. Peak A_1 has been ascribed to the underpotential deposition of sulphide by Woods and co-workers [8]. When the upper potential limit exceeds -0.2 V, the appearance of the anodic current peaks A_2 and A_3 is related to

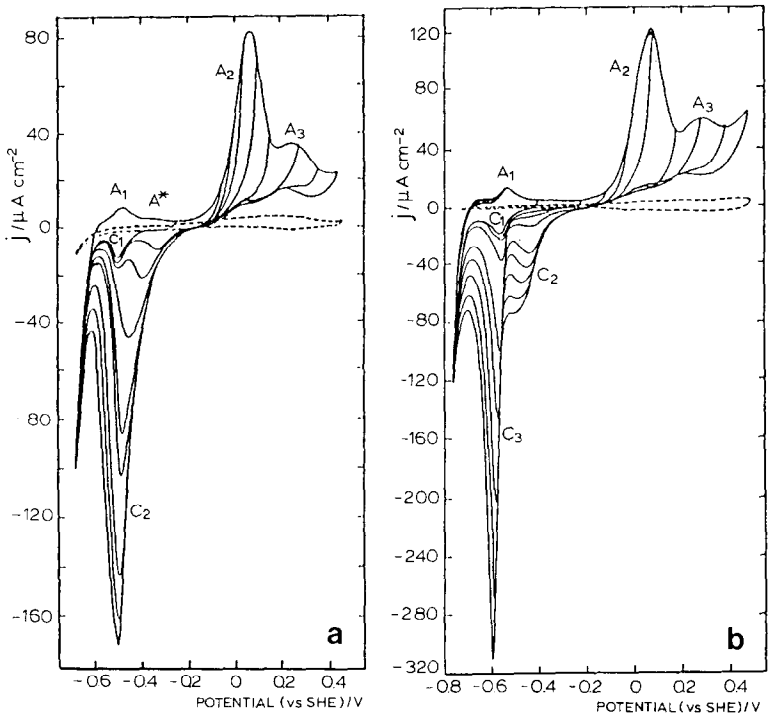

Fig. 1. Voltammograms run at 20 mV/s covering different upper reversing potentials. Gold electrode in sodium tetraborate solution; 25 °C. (a) pH 7, 3.2×10^{-3} M sulphide; starting potential −0.68 V (vs. SHE). (b) pH 9.2, 2.8×10^{-3} M sulphide; starting potential −0.74 V (vs. SHE).

the formation of sulphur multilayers [8]. The heights of peaks A_2 and A_3 depend on the pH and the sulphide concentration in the solution, although it should be noted that peak A_3 cannot be observed for sulphide concentrations lower than 5×10^{-4} M.

During the reverse scan there are three different contributions to the cathodic current, the process being better defined at pH 9.2. In addition to peak C_1, which appears under the conditions already described, a large cathodic contribution, peak C_2, is observed, corresponding to the electroreduction of sulphur multilayers to polysulphide species [8], followed by peak C_3, which has been assigned to the electroreduction of polysulphide to sulphide [8]. The stripping of sulphur deposited on top of the first adsorbate layer at pH 7 increases in charge, and correspondingly its peak potential shifts negatively as the upper potential limit is set to more positive values. Thus, for upper reversing potentials greater than −0.05 V, the height of current peak C_2 largely exceeds that of current peak C_1, and a large single cathodic peak results instead of the two peaks recorded at intermediate potential amplitudes. In this case, peak C_1 can be detected only by differential reflectivity owing to its higher reversibility with respect to that of the multilayer electroreduction (see

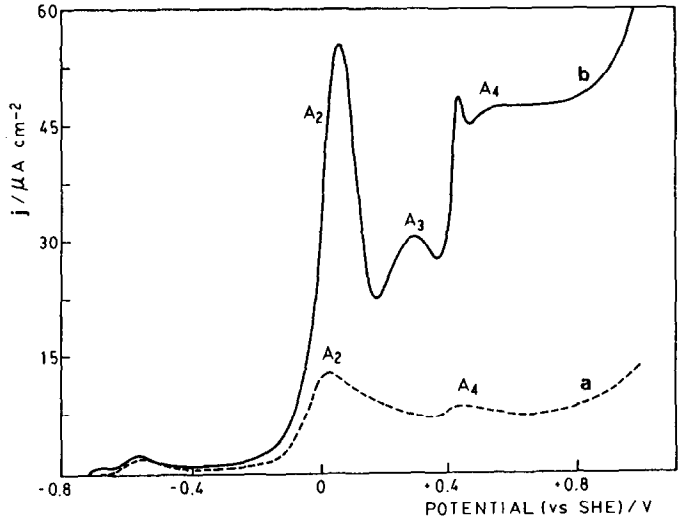

Fig. 2. Voltammograms run at 3 mV/s covering the sulphide ion electro-oxidation potential range. Gold electrode in sodium tetraborate solution, pH 9.2, containing (a) 2×10^{-4} M and (b) 2×10^{-3} M sulphide. 25°C.

Section III.2). The fact that the entire voltammetric charge on the reverse scan is smaller than that on the positive-going potential scan has been accounted for in terms of soluble species formed simultaneously with the growing of sulphur multilayers [6,8].

The effect of sulphide concentration on the positive-going potential voltammogram, at pH 9.2 and low sweep rates, is shown in Fig. 2. Thus, at 2×10^{-4} M sulphide, the deposition of sulphur begins at about -0.2 V (peak A_2), followed by a current peak or limiting current (A_4) at 0.4 V. The shape of peak A_2 for 2×10^{-4} M sulphide (Fig. 2, curve a) is consistent with the irreversible electrochemical oxidation of sulphide ion under diffusion kinetic control. When the concentration of sulphide is raised to 2×10^{-3} M, the voltammogram displays an additional peak, A_3, at 0.28 V (Fig. 2, curve b) and a limiting current from 0.45 V upwards up to the potential region where the oxidation of sulphur to sulphate takes place [4]. In addition, the diffusion kinetic control of peak A_2 is no longer observed, as $j_{\text{peak } A_2}$ does not increase proportionally to sulphide concentration (Fig. 2). Under these conditions, the shape of peak A_2 can be described better in terms of the formation of a sulphur-containing layer whose electrical conductivity decreases as the film becomes thicker.

The process related to peak A_3 cannot be observed at low sulphide concentrations or at high sweep rates. Furthermore, the height of peak A_3 was found to depend on solution stirring, as should be expected for chemical dissolution of the sulphur layer.

The voltammetric data indicate the potential ranges where the different processes

related to sulphide–gold interactions and sulphur multilayer formation take place. On the basis of these results, the appropriate conditions for in-situ reflectance measurements were selected. Accordingly, the following presentation of the results is made by considering separately the optical response of the system in the potential ranges where the two major processes are observed.

(III.2) Sulphide electrosorption

(III.2.1) In-situ visible reflectance spectroscopy

The electrosorption/electrodesorption of sulphide species occurs at potentials lower than -0.3 V (Fig. 1) and is related, at least, to the conjugated pair of peaks A_1/C_1. In this case, the differential reflectance, plotted as $\delta R/R$ vs. the electrode potential curves, was determined at two photon energies, 2.5 and 1.82 eV, for 1.35×10^{-4} M sulphide (Fig. 3) as the potential was cycled slowly from -1.0 to -0.25 V. The results show an adsorption process, A'_1, which occurs at potentials negative to peak A_1. The species involved in A'_1 may account for the shift of the threshold potential of the HER to more positive potential values. The optical profile resulting for the positive-going potential scan shows a broad differential reflectance peak A'_1 at ca. -0.66 V overlapping to a large extent the sharper peak A_1 centred at -0.48 V. This peak correlates with peak A_1 on the voltammogram (Fig. 1a) and therefore involves a charge-transfer process. Peak A_1 is followed by a rapid decrease in reflectance to a very low value in the vicinity of -0.25 V. The dependence of the

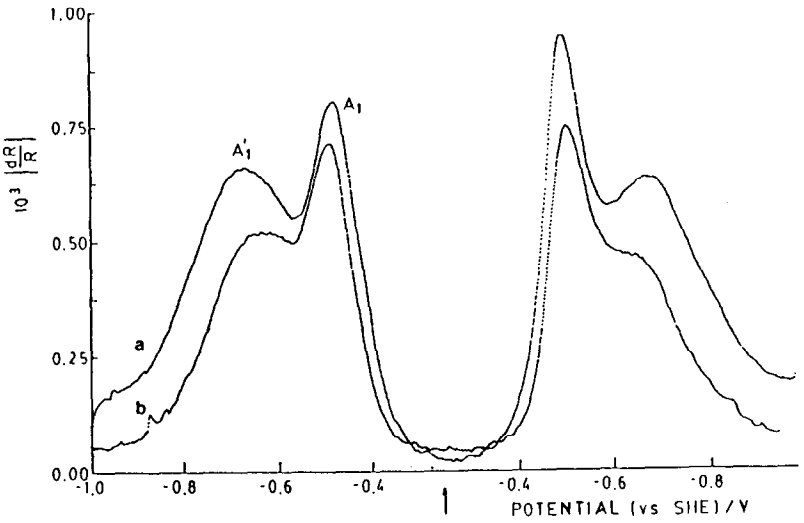

Fig. 3. Differential reflectance vs. electrode potential curves for 1.35×10^{-4} M sulphide in sodium tetraborate, pH 7, 25 °C. Starting potential -1.0 V; upper reversing potential -0.25 V (indicated by the arrow). Ac potential amplitude, $\delta E = 50$ mV_{pp}. Modulation frequency $f = 11$ Hz. Angle of incidence $\phi = 59°$, p-polarized light; (a) 2.5 eV; (b) 1.82 eV.

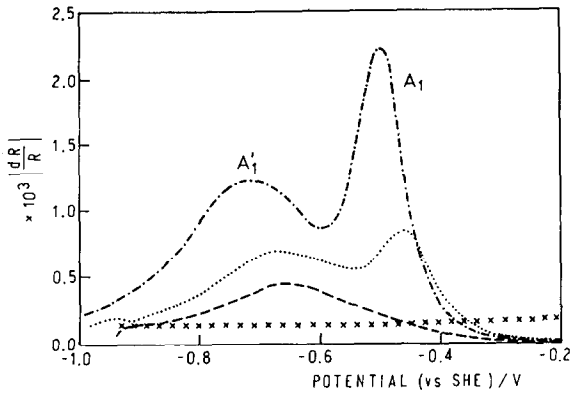

Fig. 4. Differential reflectance vs. electrode potential plots. Different sulphide concentrations, pH 7, 2.5 eV. (— — —) 5.0×10^{-5} M, (·····) 3×10^{-4} M and (·-·-·) 3×10^{-3} M sulphide in sodium tetraborate. Potential range between −1.0 and −0.2 V. $f = 11$ Hz, 25 °C. A blank run is included for comparison.

differential reflectance on the electrode potential is similar for the two photon energies, i.e. 2.5 and 1.82 eV, although peak A_1', in contrast to peak A_1, becomes somewhat better resolved at 2.5 eV, i.e. at the absorption edge of gold.

On reversing the potential sweep, almost the same differential reflectance vs. electrode potential profile is obtained, although in this case the height of peak C_1 increases slightly, presumably because of the accumulation of species associated with peak A_1. These results demonstrate that the adsorption of sulphide species on gold commences at potentials inside the HER potential region. However, the onset of the HER does not distort the optical measurements, as can be observed on the blank run made at 2.5 eV (see Fig. 4).

The influence of the sulphide concentration on the adsorption of sulphide species on gold is shown in Fig. 4. For 5×10^{-5} M and $f = 11$ Hz, only peak A_1' can be observed, whereas at higher concentrations both peaks, A_1' and A_1, are present. The height of peak A_1 displays a stronger dependence on the sulphide concentration than that of peak A_1', although the potentials of both maxima shift negatively upon increasing the sulphide concentration. This behaviour is typical of adsorption–desorption processes [19]. Therefore, it appears that the occurrence of peak A_1 requires a certain critical surface concentration of the first adsorbate, peak A_1'.

(III.2.2) Adsorption isotherm

Chronocoulometry was used to evaluate the equilibrium coverage by adsorbates involved in the processes giving rise to peaks A_1' and A_1 at pH 7. For this purpose, 1×10^{-3} M sulphide concentration in the supporting electrolyte solution was employed. The perturbing potential programme used for the potentiostatic steps is included as an inset in Fig. 5. The sequence of potential steps was designed so as to have, for a given potential, an adsorbate-free gold electrode both at the beginning and at the end of the measurement with a minimum of interference from the HER.

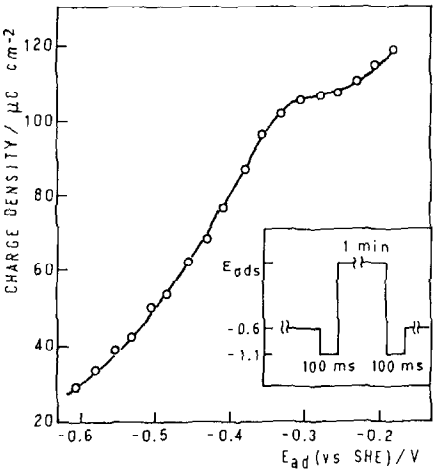

Fig. 5. Charge density vs. adsorption potential plot for adsorbed sulphide species; 1×10^{-3} M sulphide in sodium tetraborate, pH 7, 25 °C. The inset shows the measuring potential programme.

Accordingly, commencing from −0.6 V, the electrode was cleaned of adsorbate by stepping the potential to −1.1 V for 100 ms, then to E_{ads} for 1 min to reach equilibrium (see below), and finally stepped back to −1.1 V to record the current transient. After 100 ms, the potential was set back to −0.6 V to avoid the formation and growth of hydrogen bubbles. The complete electrodesorption current transient, obtained by stepping the potential between E_{ads} and −1.1 V, was integrated as a function of time and the resulting charge vs. time curve was extrapolated to zero time to obtain the amount adsorbed at E_{ads} and to eliminate the HER faradaic contribution [20]. The time necessary to achieve adsorption equilibrium was determined by measuring the adsorption kinetics in 1×10^{-3} M sulphide. Hence, the charge adsorbed at various times between 0.2 s and 1.5 min was measured as described above. In this case, adsorption equilibrium was found to be established at ca. 30 s.

Values of E_{ads} were chosen in the potential range comprised between the threshold potential of the HER and that of the formation of sulphur multilayers. The equilibrium charge density vs. electrode potential plot (Fig. 5) reveals an initial charge density of 28 $\mu C/cm^2$ at −0.6 V which can be assigned to peak A'_1, and a plateau at potentials higher than −0.35 V which correlates with the potential of peak A_1 determined either voltammetrically or through the differential reflectance vs. electrode potential plots.

(III.3) Multilayer formation

At potentials higher than −0.2 V (Figs. 1 and 2), the deposition of sulphur multilayers takes place, involving several processes whose complexity increases according to the sulphide concentration.

(III.3.1) Optical detection of polysulphide intermediates

The optical response of the system in the form of differential reflectance (in-phase component) vs. electrode potential in the range −1.05 to +0.45 V for a photon energy equal to 2.5 eV is depicted in Fig. 6 for two sulphide concentrations. For 2×10^{-4} M sulphide (Fig. 6, curve a), in addition to the features already described for the electroadsorption region, the differential reflectance vs. electrode potential plot presents two small waves in the multilayer region nearly symmetric with respect to the upper reversing potential. In this case, the sign of the optical signal in the range 0.1–0.45 V is opposite to that found in the sulphide electroadsorption region, i.e. the light intensity reflected at the positive end of the modulation is larger (less absorption) than that detected at the negative extreme. Polysulphides are known to absorb light at 2.5 eV [21] and have been proposed as intermediates [8] in the oxidation of sulphide to sulphur according to the reaction sequence

$$x\ S^{2-} \rightarrow (S_x^{2-})_{int} \rightarrow (x\ S^0)_{ads}$$

where int stands for the S_x^{2-} species at the interface and ads denotes adsorbed sulphur. The diffusional characteristics of the oxidation of sulphide to polysulphide were confirmed, for low sulphide concentrations such as 2×10^{-4} M, by observing the corresponding optical transients (integral measurements) at 2.5 eV by stepping the potential from −0.64 to +0.24 V (Fig. 7). The curve shows initially a rapid change of reflectivity arising from the electroreflectance effect of gold, followed by a

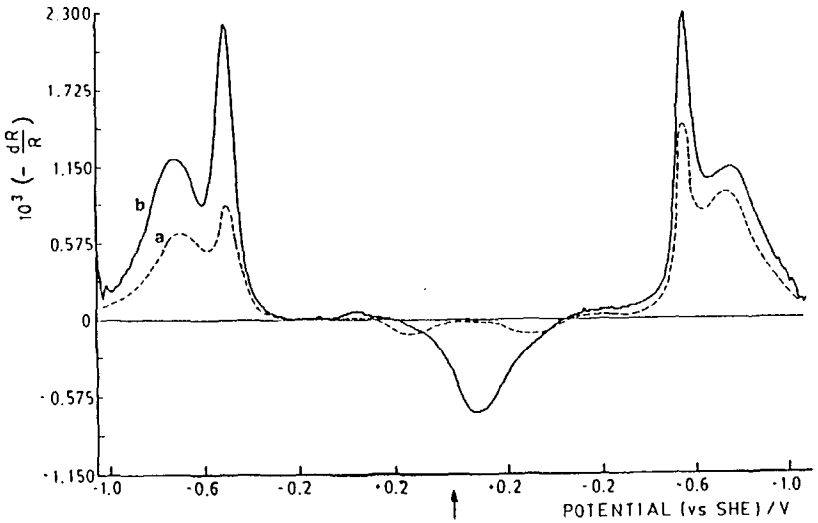

Fig. 6. Different reflectance (in-phase) vs. electrode potential curves at 2.5 eV. The potential was swept cyclically from −1.05 to +0.45 V; $\delta E = 50$ mV, $f = 11$ Hz, $\phi = 59°$, p-polarization. (a) 2×10^{-4} M and (b) 3.2×10^{-3} M sulphide in sodium tetraborate solution, pH 7, 25 °C. The upper reversing potential is indicated by the the arrow on the potential axis.

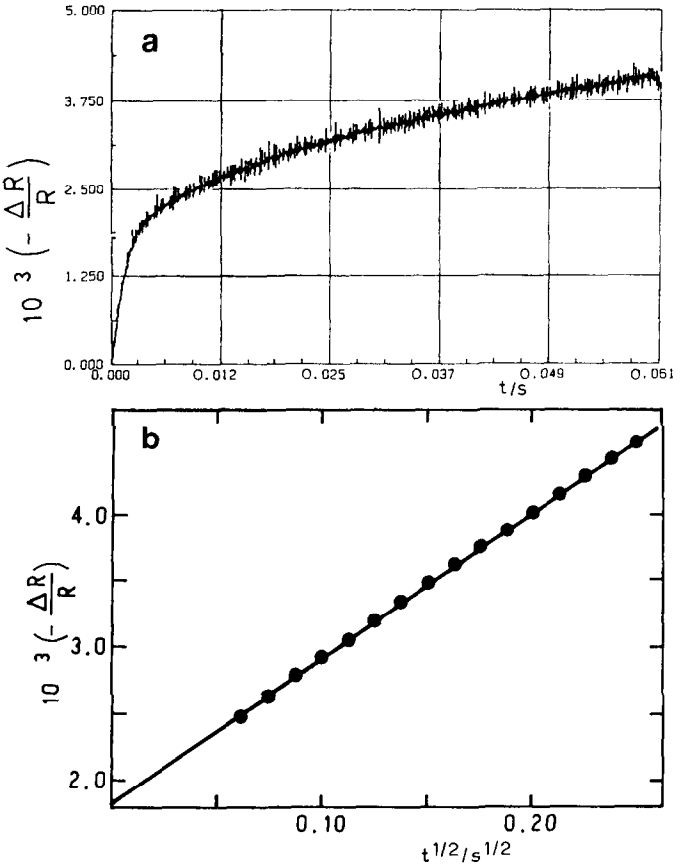

Fig. 7. Time dependence of the integral change of reflectance accompanying the formation of sulphur multilayers. Potential step from −0.64 to +0.24 V, 2×10^{-4} M sulphide, pH 7, 25°C. (a) Optical transient; (b) $\Delta R/R$ vs. $t^{1/2}$ relationship. The straight line intercept arises from the change in the electroreflectance effect of gold between the two potentials employed.

gradual loss of reflectivity brought about by the deposition of sulphur which displays a linear decrease with the square root of time (Fig. 7b). With a view to comparing these results with those of a similar model system, a 2×10^{-3} M $K_4[Fe(CN)_6]$ solution and a platinum electrode were used. In this case, the following electrochemical reaction takes place:

$$[Fe(CN)_6]^{4-} \text{ (transparent at 3 eV)} \leftrightarrow [Fe(CN)_6]^{3-}_{int} \text{ (light absorbing at 3 eV)} + e^-$$

yielding strongly light-absorbing ferricyanide ion as the product. The corresponding $\delta R/R$ vs. electrode potential plot at 3.0 eV (Fig. 8) is determined exclusively by the amount of ferricyanide ion modulated at the interface under diffusion-controlled conditions [22]. The sign of the optical signal corresponds to a greater light absorption at the positive limit of the modulation where the ferricyanide ion is

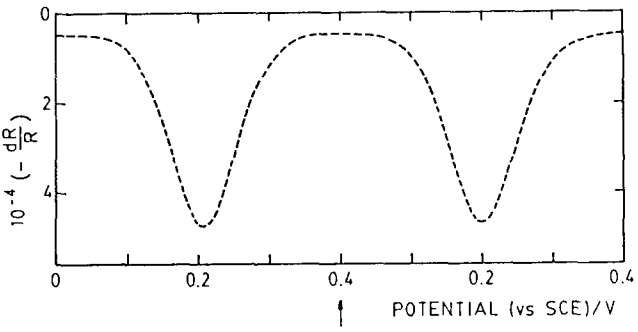

Fig. 8. Differential reflectance vs. electrode potential plot at 3.0 eV. Pt/0.5 M NaF+2×10^{-3} M $K_4[Fe(CN)_6]$; 3 eV; $\delta E = 50$ mV_{pp}; $f = 11$ Hz; $\phi = 59°$; p-polarized light. The potential was swept cyclically from 0 V to 0.4 V (vs. SHE), 25 °C.

generated. This response is similar in shape to that shown in Fig. 6, curve a for the multilayer region.

On the other hand, the differential reflectance vs. electrode potential plot for 3.2×10^{-3} M sulphide (Fig. 6, curve b) provides additional information in the multilayer potential range which can be compared with that derived from the voltammetric data (Fig. 1a). In the potential range of peak A_2, the optical measurements display a small wave with the same sign as that for the adsorption process. Thereafter, the $\delta R/R$ signal changes sign at about 0.15 V and becomes greater as the electrode potential is made more positive. On reversing the potential scan at 0.45 V (see arrow in Fig. 6), the optical signal decreases to almost zero, becoming slightly negative up to the desorption region. It is worth pointing out that, in the range ca. −0.15 to −0.65 V, sulphur multilayers undergo electroreduction. However, this process, which according to voltammetry appears to be strongly irreversible, does not influence appreciably the value of the differential reflectance, as the latter can follow only the much faster processes associated with peaks A_1 and A_1'

The influence of the photon energy on the differential reflectance is shown in Fig. 9 for 3×10^{-3} M sulphide. At this relatively high sulphide concentration the formation of soluble polysulphides during the multilayer growth is favoured [23]. Besides, the optical response of the system in the multilayer potential range at 3.3 eV is better resolved than at 2.5 eV, as should be expected if polysulphide intermediates are the light-absorbing species [21]. In this potential range, the electrode becomes covered with a relatively thick sulphur-like layer.

The differential reflectance vs. electrode potential plots obtained at 3.3 eV and 11 Hz (Fig. 10) for the same solutions used in the voltammetric experiments (see Fig. 2) show a spectral resolution in the sulphide electroadsorption potential range (see Section III.2.1) at pH 9.2 that is poorer than that at pH 7 (Fig. 6). It appears that this effect is due to the slow rate of response of peak A_1 to the modulating frequency. Furthermore, for 2×10^{-4} M sulphide, pH 9.2, the differential reflec-

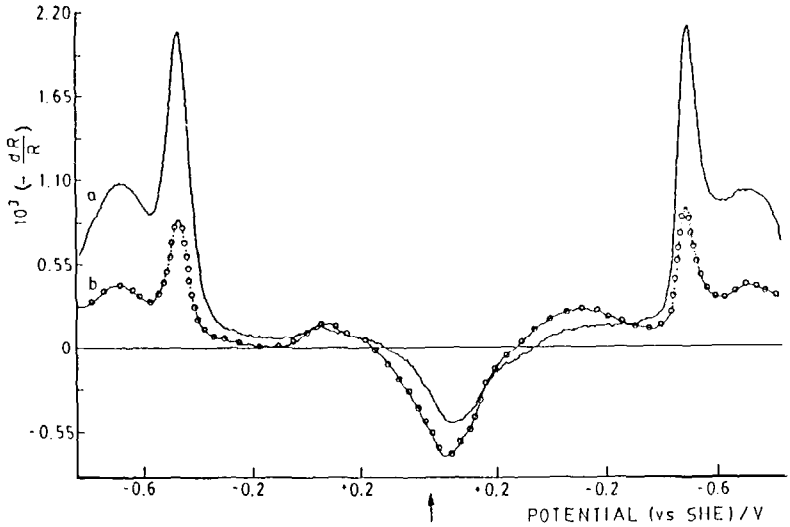

Fig. 9. Differential reflectance (in-phase) vs. electrode potential plots. 3×10^{-3} M sulphide in sodium tetraborate solution. Experimental conditions are the same as those in Fig. 6, curve b. (a) 2.5 eV; (b) 3.3 eV.

tance values resulting in the potential range of peak A_2 exhibit the same general features as those observed at pH 7, but as the potential is made more positive, the differential reflectance drops to almost zero at about 0.4 V (Fig. 10, curve a).

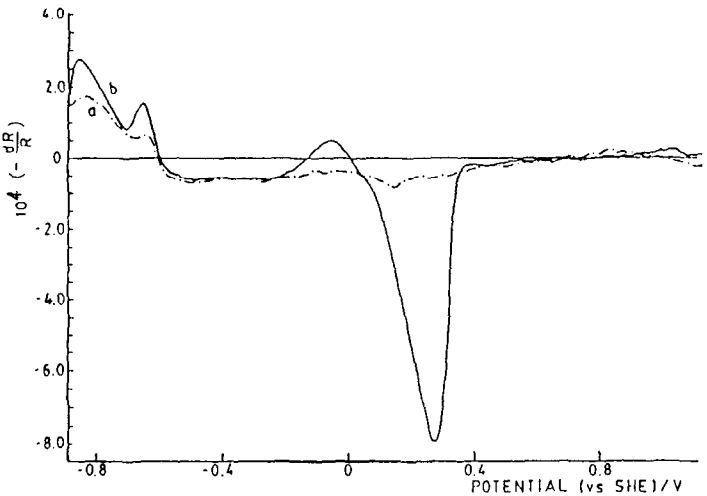

Fig. 10. Differential reflectance vs. electrode potential plots at 3.3 eV. (a) 2×10^{-4} M and (b) 2×10^{-3} M sulphide in sodium tetraborate solution, pH 9.2. The potential was scanned from -0.72 to $+1.0$ V.

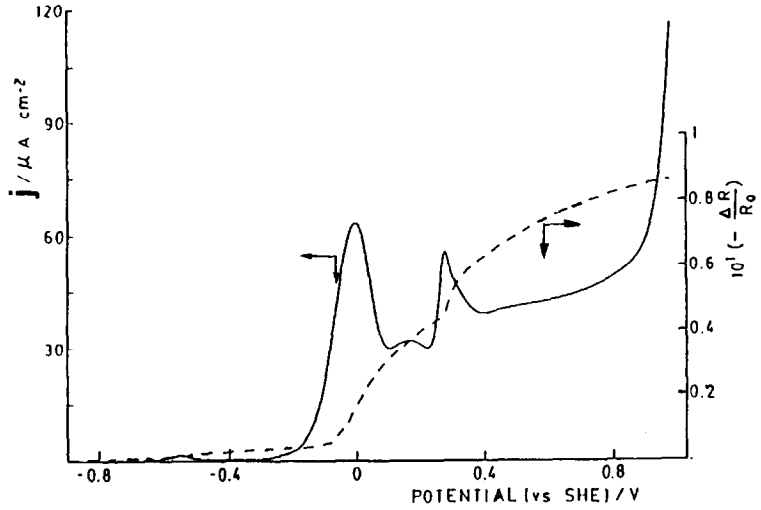

Fig. 11. Integral reflectance vs. electrode potential plot (normalized to the reflectance in the sulphide electroadsorption region) at 3.3 eV and voltammogram run at 3 mV/s. 2×10^{-3} M of sulphide in sodium tetraborate, pH 9.2, 25 °C.

For 2×10^{-3} M sulphide, the differential reflectance in the potential range of peak A_3 goes through a change in sign, from negative to positive (Fig. 10, curve b), and it grows rapidly to reach a peak value of about 8×10^{-4} for $E\approx0.3$ V. However, on increasing the potential further, the differential reflectance falls abruptly to a negligible value. The potential range where these changes can be observed coincides with that of the region where a limiting current appears in the corresponding voltammogram (Fig. 2).

Further details about the different processes associated with the formation of multilayers can be derived from integral reflectance, $(R-R_0)/R_0$, measurements (Fig. 11). Changes in the integral reflectance obtained at slow potential sweep rates were normalized to the value R_0 observed in the sulphide electroadsorption potential range, where changes in the reflectance are comparatively negligible. The integral reflectance value decreases monotonically as the potential moves towards more positive values in the region of peaks A_2 and A_3. However, when the potential enters the range of peak A_4, an abrupt change in the integral reflectance can be observed. It should be mentioned that in the region spanned by peak A_4 and in the subsequent limiting current range, the multilayer is continuously growing and can be stripped off the surface only when the applied potential reaches the value where the formation of gold oxide takes place [4].

(IV) DISCUSSION

The voltammetric behaviour of sulphide species on gold shows, in accord with previous reported data [6,8], that there are at least two distinguishable regions. The

first one, at lower potentials, comprises the electroadsorption of sulphide species, the charge involved in this case being less than that corresponding to a sulphur monolayer. Differential reflectance measurements proved to be particularly suitable for detecting the sulphide electroadsorption stages. The second region, found at higher potentials, implies the formation of sulphur multilayers and the appearance of soluble sulphur-containing species.

(IV.1) Sulphide electroadsorption

Voltammetric data indicate that sulphide electroadsorption on gold occurs at potentials below the reversible potential of the S^{2-}/S^0 redox couple [23]. In the present case, the maximum voltammetric charge density related to the sulphide electroadsorption on gold is ca. 107 $\mu C/cm^2$, and the corresponding reaction appears to behave as a nearly reversible process, a conclusion drawn from the appearance of the peaks A_1/C_1 (Fig. 1) in the range -0.6 to -0.4 V. The differential reflectance measurements vs. electrode potential plots (Figs. 3 and 4) confirm the existence of voltammetric peaks A_1 and A_1' corresponding to a reflectance change due to the formation of adsorbed sulphide species. For 3×10^{-3} M sulphide, this process occurs entirely in the HER potential range and the corresponding charge density, derived by extrapolating the adsorption charge to -0.6 V (Fig. 5), is ca. 28 $\mu C/cm^2$, i.e. much smaller than the charge density corresponding to peak A_1.

When either neutral or slightly alkaline solutions are employed, the predominant species at the interface is SH^- because the pK value for the equilibrium

$$H_2S(sol) \leftrightarrow H^+ + HS^- \quad (1)$$

is about 7. Accordingly, the reaction related to peak A_1' can be written as an ionic adsorption such as

$$Au + SH^- \rightarrow Au\text{–}(SH^-)_{ads} \quad (2)$$

Comparison of curves b in Figs. 9 and 10 in the potential range of peak A_1' indicates that the intensity of the latter does not depend on the bulk pH value but, as it can be observed with the same intensity at pH 7 and 9.2, it should depend on the local pH.

The width of the $Au\text{–}(SH^-)_{ads}$ peak indicates the presence of interactions in the adsorbed layer, as should be expected for the adsorption of charged species. The capacitive behaviour of peak A_1' is shown by the shifting of the peak potential to more negative values with increasing sulphide concentration in solution. On the other hand, process (2) is better resolved at 2.5 eV (absorption edge of gold) than at 1.82 eV (Fig. 3), and, besides, the shape of the electroreflectance spectrum of gold, measured as $\delta R/R$ vs. wavelength, is not significantly altered when the bias potential is set to the peak value (only its magnitude is enhanced, leading to more negative values). This behaviour can be accounted for by assuming a weak adsorbate–gold interaction.

Peak A_1 which has been detected both voltammetrically and optically is likely to involve a charge-transfer process. The spectrum of gold, clearly distorted by the presence of the adsorbate, can be detected even at 1.82 eV, i.e. away from the absorption edge of gold. This behaviour points to a relatively strong adsorbate–gold interaction, probably through the formation of a covalent bond. The species giving rise to peak A_1 are likely to be adsorbed uncharged, and therefore the peak sharpness may arise from the lack of strong interactions. On the whole, the features displayed by peak A_1 are quite distinctive from those shown by maximum A'_1.

The process giving rise to peak A_1 can be described as

$$Au\text{–}(SH^-)_{ads} \rightarrow Au\text{–}S + H^+ + 2\,e^- \qquad (3)$$

involving the formation of a Au–S surface compound presumably at the submonolayer level, as deduced from the charge density value.

The adsorbate in this case can be better described as a gold sulphide, as concluded from XPS data [8]. As can be seen from peak A_1 (Fig. 1), the charge involved in the formation of the gold sulphide layer remains practically independent of the pH. However, the modulated optical response of peak A_1 at the same frequency shows a slower response at pH 9.2 than at pH 7 (curves b, Figs. 9 and 10). This behaviour can be accounted for by a surface process such as that indicated by reaction (3), where the rate of the backward reaction should depend on the proton concentration at the interface. Reaction (3) appears to be able to modify the electronic properties of gold, giving rise to a rather large effect on its electroreflection coefficient. It is worth noting that this effect is somewhat similar to that found earlier for the adsorption of other sulphur-containing species on Au [24].

(IV.2) Multilayer formation

The multilayer formation takes place in the relatively wide potential range covering peaks A_2, A_3 and A_4. From the electrochemical data, the imbalance of the anodic to the cathodic voltammetric charge indicates the presence of soluble species as reaction intermediates (e.g. in Fig. 1b, $Q_a = 2270\ \mu C/cm^2$ and $Q_b = 1640\ \mu C/cm^2$). Besides, there is a clear similarity in the optical behaviour of the ferrocyanide/ferricyanide system with that obtained during the deposition of sulphur in the multilayer range (Fig. 6, curve a), the only differences being a change in sign in the optical response and a scale factor. This analogy can be explained if the electrical modulation is perturbing the transformation of polysulphide to sulphur, the concentration of polysulphide being determined by the rate of diffusion of sulphide ion to the interface. The difference in the sign of the optical signal is to be expected if, at the negative limit of the modulation, the polysulphide ions are absorbing light much more strongly than the deposited sulphur layer. Thus, for 2×10^{-4} M sulphide, the differential reflectance spectrum shows that polysulphide species are formed as soluble intermediates under diffusion control. The latter is supported by the shape of the optical transient (Fig. 7, curve a) accompanying the electrodeposition of sulphur, the final product in the multilayer formation. The

electrochemical measurements and the differential reflectance–electrode potential curves in the potential range from −0.2 to 0.45 V (curves a, Figs. 6 and 10) can be explained through a reaction scheme such as

$$\text{Au–S} + x\ \text{HS}^- + x\ \text{OH}^- \rightarrow (\text{Au–S})(\text{S}_x^{2-})_{\text{int}} + x\ \text{H}_2\text{O} + 2(x-1)\ \text{e}^- \quad (4)$$

$$(\text{Au–S})(\text{S}_x^{2-})_{\text{int}} \rightarrow (\text{Au–S})(\text{S}_x^0)_{\text{ads}} + 2\ \text{e}^- \quad (5)$$

where $x \geqslant 2$, and int stands for interface. Step (4) corresponds to the formation of the intermediate S_x^{2-} at the interface which reacts further to yield the S^0 multilayers as formally indicated through reaction (5).

For 3×10^{-3} M sulphide and at low sweep rates the optical measurements in the potential range of voltammetric peak A_2 (Fig. 6, curve b) display a small wave with the same signs as that for the adsorption process. This change in the differential reflectance is probably brought about by the beginning of the deposition of sulphur, at the leading edge of the voltammetric peak A_2, and arises from either the loss of reflectivity of the gold electrode or the absorption of light at the sulphur layer itself.

Polysulphides can be formed either through reaction (5) or through the following reaction [6,8]:

$$(\text{Au–S})\text{S}_x^0 + \text{SH}^- \rightarrow (\text{AuS})\text{S}_{x-n} + \text{S}_{n+1}^{2-} \qquad (x \geqslant n) \quad (6)$$

The polysulphides formed through chemical reaction (6), S_{n+1}^{2-}, may account for the steep increase in the positive differential optical signal (absorption of light at the negative end of the modulation) (Fig. 6, curve b, and Fig. 9) just before the upper reversing limit in the potential region of voltammetric peak A_3. This assumption is supported by the fact that peak A_3 is not observed either at low sulphide concentrations or at high sweep rates. Besides, the peak height was found to depend on solution stirring. The chemical production of polysulphides is detected clearly at 3.3 eV (Figs. 9 and 10).

It is rather surprising that at potentials more positive than 0.47 V (peak A_4), in spite of the presence of an apparently insulating layer of sulphur, the system can still sustain relatively high anodic currents. The presence of defects or pinholes in this layer has been proposed to account for the mechanism of other similar systems which present extended charge transfer [25]. However, with regard to the abnormally high electronic conductivity of the layers, it is possible to look for some other explanations. The change in resistance taking place at peak A_4 may arise from the incorporation of polysulphides into the structure of the adsorbed layer, yielding long polysulphur chains. Besides, in a report on the adsorption of sulphur on gold in 1 M KOH at 0.7 V (vs. RHE) [26], in-situ Raman spectra were interpreted as originating from polysulphide species adsorbed on the gold electrode. Negative-going potential voltammograms at pH 9.2 for 2.8×10^{-3} M sulphide (Fig. 1b) support the view of having adsorbed polysulphide chains, as the reverse sweeps started in the 0.35–0.45 V range present a rather large peak for the electroreduction of polysulphide to sulphide, whereas the peak corresponding to the electroreduction of adsorbed sulphur to polysulphide is rather small. It should be noted that the process

related to peak A_4 and the ensuing limiting current involve two electrons per reactant species, as determined by potentiostatic steps from potentials where the electrode was adsorbate-free.

Feher and Munzner [27], in an attempt to interpret the absorption spectra of sulfanes, showed that the simple free electron model commonly used for conjugated organic systems can be used successfully to explain the positions and intensities of the low energy bands of these compounds as a function of the chain length. These findings pointed out the presence of a conjugated system extending over the entire length of the polysulphur chain with delocalized orbitals playing an important role in determining the spectral properties of ions of the type S_nS^-, n being the number of atoms of zero-valent sulphur per polysulphide ion. The steep fall in reflectivity (integral) starting at peak A_4 may arise from the lengthening of the chains as the film grows thicker, since the chain bands are red-shifted and their intensity increases with n.

The increase in current at high positive potentials may also be explained through the formation of sulphur clusters of the type S_4^{2+}, S_8^{2+} and S_{19}^{2+} [28] at the surface. These clusters might be formed at high positive potentials, leading to the abrupt increase in current observed, probably due to the formation of channels that leave conducting domains in the film layer.

(IV.3) Influence of adsorbed sulphide on the HER

It is known that small amounts of sulphide species bring about an electrocatalytic effect on the HER on Ag, Fe and Ni (110) [5,29]. A similar behaviour is found for the HER on gold in neutral and slightly alkaline solutions containing Na_2S, as can be seen by comparing the voltammograms in Fig. 1 for sulphide-free with those for sulphide-containing solutions.

The process related to peak A_1' observed by means of differential reflectance spectroscopy (Figs. 3 and 4) indicates a direct relationship between the first electroadsorption stage of sulphide species at the submonolayer level and the HER electrocatalytic effect. Thus, if the discharge of the water molecule to give $Au-H_{ads}$ is the rate-determining step, the catalysis may be promoted by the presence of the species $Au-(SH^-)_{ads}$ through the increase of the Me–H bond strength. This mechanism has been proposed tentatively to explain the enhancement of the HER on Ag [5] taking into account results from the gas phase, where the energy of the Me–H bond was found to be modified by co-adsorption [30].

(IV.4) Conclusions

The adsorption of sulphide was found to begin at rather negative potentials, inside the HER region. This reaction is clearly catalysed by the presence of sulphide species on the gold. Differential reflectance vs. electrode potential curves show two main stages in the adsorption of sulphide on gold, peaks A_1' and A_1. Peak A_1' seems to be related to the modulation of the charge on the metal, and consequently it is

linked to the electroreflectance spectrum of gold. The concentration dependence of this peak follows that expected for an adsorption–desorption process.

On the contrary, the process giving rise to peak A_1 in the differential reflectance spectrum shows up only after the surface concentration of adsorbates has reached a certain critical value. Process A_1 is affected strongly by the frequency of the potential modulation and may be assigned to a change in the differential reflectance brought about by a variation in the degree of surface coverage through a charge-transfer process. Optical measurements in the multilayer potential region allowed us to detect polysulphide species at the interface. For 2×10^{-4} M sulphide, the differential reflectance vs. electrode potential curves at 3.3 eV show that polysulphides are produced on the forward scan, under diffusion-controlled kinetics. On the other hand, for 3×10^{-3} M sulphide, the optical signal related to the formation of polysulphides increases greatly in the potential region of peak A_3 owing to a chemical reaction between the sulphide in solution and the sulphur layer on the electrode yielding soluble polysulphide species. The chemical dissolution of sulphur may account for the loss of passivity observed. The incorporation of polysulphide into the structure of the deposited sulphur layer can lead to long polysulphide chains with probably a high electronic conductivity. Accordingly, the steep fall in the integral reflectance at the potential of current peak A_4 may arise from the lengthening of the chains as the film becomes thicker, since the bands of polysulphide chains are red-shifted and their intensity increases with the number of sulphur atoms in the structure.

ACKNOWLEDGEMENTS

This research project was supported financially by the Consejo Nacional de Investigaciones Científicas y Técnicas, the Comision de Investigaciones Científicas de la Provincia de Buenos Aires and the Regional Scientific Programme of the Organization of American States (OAS).

REFERENCES

1 P.E. Richarson, S. Srinivasan and R. Woods (Eds.), Proc. Int. Symp. Electrochemistry in Mineral and Metal Processing, The Electrochemical Soc., Pennington, NJ, 1984.
2 P.L. Allen and A. Hickling, Trans. Faraday Soc., 53 (1957) 1626.
3 M. Farroque and I.Z. Fahidy, J. Electrochem. Soc., 124 (1977) 1191.
4 D.G. Wierse, M.M. Lohrengel and J.W. Schultze, J. Electroanal. Chem., 92 (1978) 121.
5 C. Nguyen Van Huong, R. Parsons, P. Marcus, S. Montes and J. Oudar, J. Electroanal. Chem., 119 (1981) 137.
6 I.C. Hamilton and R. Woods, J. Appl. Electrochem., 13 (1983) 783.
7 E. Lamy Pitara and J. Barbier, Electrochim. Acta, 31 (1986) 717.
8 A.N. Buckley, I.C. Hamilton and R. Woods, J. Electroanal. Chem., 216 (1987) 213.
9 B.L. Wheeler and N. Hackerman, J. Phys. Chem., 92 (1988) 1601.
10 Y. Berthier, M. Perdereau and J. Oudar, Surf. Sci., 36 (1973) 225.
11 H.P. Bonzel and R. Ku, J. Chem. Phys., 59 (1973) 1641.
12 T.E. Fischer and S.R. Kelemen, Surf. Sci., 69 (1977) 1.

13 M. Auer, H. Leonhard and K. Hayek, Appl. Surf. Sci., 17 (1983) 70.
14 M. Perdereau and J. Oudar, Surf. Sci., 20 (1970) 80.
15 M. Kostelitz, J.L. Domange and J. Oudar, Surf. Sci., 34 (1973) 431.
16 V. Svetlicic, V. Zutic, J. Clavilier and J. Chevalet, J. Electroanal. Chem., 233 (1987) 199.
17 R.C. Salvarezza, H.A. Videla and A.J. Arvia, Corros. Sci., 22 (1982) 815.
18 R.O. Lezna, N.R. de Tacconi, J, Rappallini and A.J. Arvia, An. Asoc. Quim. Argent., 76 (1987) 25.
19 B.B. Damaskin, O.A. Petrii and V.V. Batrakov, Adsorption of Organic Compounds on Electrodes, Plenum Press, New York, 1971.
20 J. Richer and J. Lipkowski, J. Electrochem. Soc., 133 (1986) 121.
21 W. Giggenbach, Inorg. Chem., 11 (1972) 1201.
22 J.W. Strojek and T. Kuwana, J. Electroanal. Chem., 16 (1968) 471.
23 R. Woods, D.C. Constable and L.C. Hamilton, 173rd Meeting of the Electrochemical Society, Atlanta, May 1988, Extended Abstracts, p. 536.
24 R.O. Lezna, N.R. de Tacconi and A.J. Arvia, J. Electroanal. Chem., 255 (1988) 251.
25 Symposium on Critical Issues in the Structure and Chemistry of Organic Monolayers at Electrode Surfaces at the 171st Meeting of the Electrochemical Society, Philadelphia, 10–15 May 1987.
26 H. Baltruschat, N. Stand and J. Heitbaum, J. Electroanal. Chem., 239 (1988) 361.
27 F. Feher and H. Munzer, Chem. Ber., 96 (1963) 1131.
28 J. Lewis, Chem. Br., (1988) 795.
29 P. Marcus and J. Oudar, C.R. Acad. Sci., 284 (1977) 959.
30 G. Wedler and F.J. Broker, Z. Phys. Chem., N.F., 75 (1971) 299.